Master's Thesis
Semester 9

Interacting quantum walk on a 1D Su-Schrieffer–Heeger model

Submitted by

S. Gauthameshwar
Int. MSc 2018
National Institute of Science Education and Research

Under the guidance of

Prof. Tapan Mishra
Reader-F

School of Physical Sciences
National Institute of Science Education and Research
Bhubaneshwar

MSc Thesis progress report

Declaration

This is to declare that the thesis entitled "Interacting quantum walk on a 1D Su-Schrieffer–Heeger mode", submitted by me to the National Institute of Science Education and Research, Bhubaneshwar, as a part of my Master's thesis, is a bonafide work carried out by me under the supervision of Dr. Tapan Mishra. The content of this thesis, in full or in parts, have not been submitted to any other University or Institute for the award of any degree or diploma. Works presented in the thesis are all my own unless referenced to the contrary in the thesis.

S. Gauthameshwar
5th year, Int. MSc
School of Physical Sciences
NISER, Bhubaneshwar-752050.
Signed on: 27th November, 2022

Abstract

In this first half of my thesis, we equip ourselves with the necessary computation tools and background knowledge to explore topology and its introduction to physical systems. We shall be working on the Su-Schrieffer–Heeger (SSH) model, in particular, to understand the topological phase transitions and the factors affecting them. We first analytically solved the closed-chain (periodic boundaries) model by computing its eigenspectrum and realized the specific topology by calculating the associated topological invariant. Later, we considered an open chain to look into the consequence of this bulk topology and found that there is an appearance of edge states. We have also computed the point at which this phase transition happens and then considered the interaction effect in my system. Since this is a more challenging model to solve, we take the help of continuous-time quantum walk formalism to simulate the system with two bosons performing quantum walks. We have used *quspin* library to get the time dynamics by the exact diagonalization method. From the simulation results, along with the formation of repulsively bound pairs for considerable interaction strength, we have found out that interaction can alter the topology of our system and can change the point at which the topological phase transition occurs. We shall take this work forward by quantifying the topological invariant, introducing disorder in our system to study localization, and trying to implement quantum walks on a quantum computer.

Contents

Chapter 1

Introduction

Topology has been a theory formulated by mathematicians since the 18th century. The simple concept of two geometries being equivalent through continuous surface transformation entered physics in the 19th century when scientists observed self-stable thee dimensional vortices in fluids. These vortices had a topological feature of linking to each other in a stabilizing way which made their existence possible[1]. This was when physicists realized the topology of a system is a distinctive feature that protects our system from losing its distinctiveness when faced with small perturbations (analogous to continuous surface deformation of our topology). Landau's theory of phase transition explains topological phase transitions as a consequence of breaking certain symmetries. Unless it does so, the matter does not undergo a phase transition. Thus, it was possible to define topological invariants and characterize our system. Exotic particles such as skyrmions[6] are a direct outcome of topology in our material. Even the Nobel prize-winning discovery

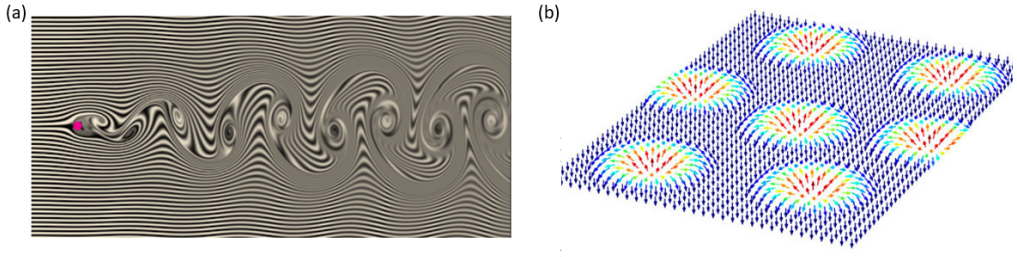

Figure 1.1: (a) A fluid simulation of Karman vortices when we introduce a particle (red) in the middle of a laminar flow. This vortex has a topological feature[2]. Figure adapted from the simulation at this website. (b) Representation of spin arrangement in the form of vortices called skyrmions that arrange electron spins in a topology-preserving way.

of the quantum Hall effect can be explained as an outcome of preserving a topological invariant that causes this quantization[3]. Topology is also used to explain fractional quantum hall effects that have been seen experimentally [7, 8]. However, the theories put to explain fractional quantum Hall effects are still mainly under debate.

After the topological insulators' discovery, the topology field gained a new wave of attraction[5]. Adding the Nobel prize contribution of David J. Thouless, F. Duncan M. Haldane, and J. Michael Kosterlitz for theoretical discoveries of topological phase transitions and topological phases of matter[4], scientists have realized it is possible to protect the conductivity of a material through topology and create what is called as surface conduction despite being insulating and dissipative in bulk. This discovery can revolutionize material science, electronic engineering, and computation. We can now have a new charge transport stabilized by topology, unlike conventional electronics with significant power dissipation while transporting charges. Physicists have already exploited this topological order of matter in quantum computation and achieved long-range entanglement without getting environmental noises [10]. This also shows the potential of topology to be extended to quantum computation and the architectures of quantum devices since one major problem with qubits, the building blocks of quantum computation, is that they are highly prone to environmental noises. Securing them with topology directly addresses this issue.

To understand what topology does to a physical system and quantify topological phase transitions to land at edge conduction, we look at the Su-Schrieffer–Heeger (SSH) model. The SSH model is a widely studied model to get introduced to this exciting field of physics for its simplistic yet informative insight into how topology effects emerge in a physical system. Even with this simplicity, the SSH model has shown many transport behaviors in poly-acetylene chains. Experimentalists have performed a quantum simulation of the SSH model in an optical lattice to show topological solitons can exist in poly-acetylene chains[9], in continuation to the original works of Su, Schrieffer, and Heeger in 1979[11].

The fact that topological insulator is a new field of research allows us to discover much-unexplored physics if we study them in detail. Only a little work has been done in the scientific community on the effect of interaction and how topology is affected in an interacting system. We shall be using quantum walks to understand this phenomenon. Quantum walks are easily implementable on an optical lattice of bosons or in a quantum

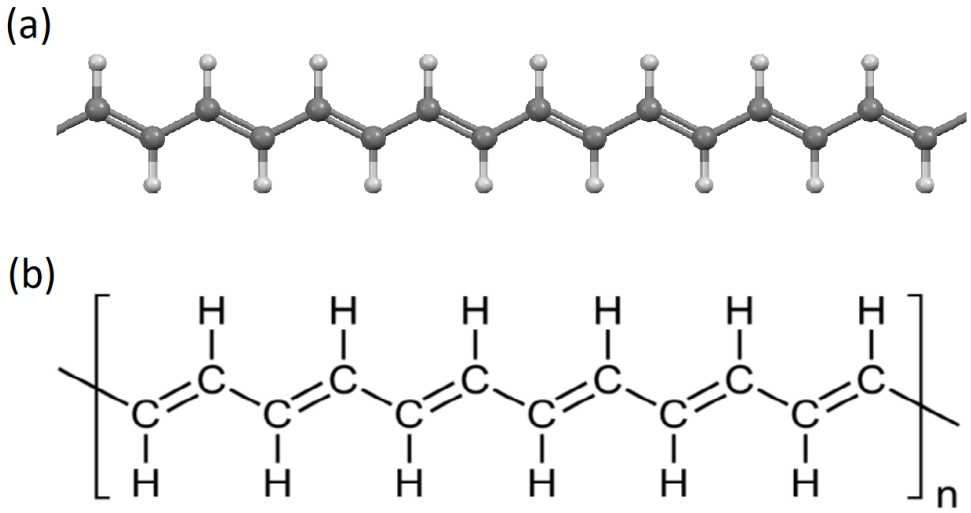

Figure 1.2: (a) A ball-stick representation and (b) the polymer formula of a polyacetylene molecule. Each carbon atom can be approximated as a discrete site where the π-electrons of the organic molecule can delocalize.

computer. Quantum walks have also widely been able to capture the features of topology[13, 14, 15, 16]. Recently, *Klauck et al.* have performed a two-particle quantum walk on the SSH model using photons and showed the existence of edge states when the system undergoes a topological phase transition[12]. Quantum walk formalism also makes the experimental realization of all my simulations feasible.

With all the above motivation set to do my project, we shall start by first understanding topology and its analogy in condensed matter systems, learn about the bulk-boundary correspondence, apply it to my system, and then study quantum walk formalism that shall help me simulate the interacting SSH model to study the time dynamics and our system's topology.

Chapter 2

Theory

2.1 Topology in mathematics

Topology is a branch of mathematics that deals with a class of objects based on their geometries. The objects of each of these classes are created through continuous surface deformation. Tearing and reattaching the surface, poking a hole, or joining it is not a continuous deformation. The famous example of a coffee cup and a donut illustrates this concept. They both fall in the same geometry class because we can do continuous transformations about the surface to transform a coffee cup into a donut.

Figure 2.1: An illustration of making a coffee cup into a donut by applying continuous transformations on the surface.

However, we cannot get a donut from a piece of paper as that involves poking a hole and introducing a discontinuity in our surface. Mathematicians have quantified this beautifully in a theorem called the Gauss-Bonnet Theorem that defines a topological invariant for the class to which our geometry belongs.

$$\frac{1}{4\pi}\oint_M \kappa dA = 1 - g \tag{2.1}$$

where the area integration is over the surface of our object, κ is the Gaussian curvature of our object that is defined at every surface point, and g is an integer that represents the number of discontinuities present in our system, which is usually holes. Eq 2.1 quantifies a topological invariant quantity g that does not change in our system when we perform any continuous transformation. So we perform this surface integral to characterize the topology of our geometry/object.

This concept will appear in our condensed matter system when we define the analog of Gaussian curvature, called the Berry curvature, and perform a surface integration over all the momentum values in the First Brillouin zone.

2.2 Adiabatic theorem for a quantum system and the Berry curvature

Before entering into the physics of our SSH model, we digress slightly to a topic in quantum mechanics to have a solid connection of topology with quantum systems.

Suppose we have a time-dependent Hamiltonian that governs the dynamics of a quantum system by following the time-dependent Schrodinger equation (TDSE):

$$i\hbar\frac{\partial|\psi(t)\rangle}{\partial t} = H(t)|\psi(t)\rangle \tag{2.2}$$

This system has an inherent difficulty in solving because the Hamiltonian itself changes with time, and that will cause complicated mixing of all instantaneous eigenstates at each point in time. Fortunately, to show us a way out of this nightmare, we have a famous theorem known as the adiabatic theorem that says our system will continue to remain in its instantaneous eigenstates (we assume it is initialized to an eigenstate at $t = 0$) if the Hamiltonian is varied slowly. With this approximation, we can say

$$H(t)|n(t)\rangle = E_n(t)|n(t)\rangle \tag{2.3}$$

where $|n(t)\rangle$ is the instantaneous eigenstate of the Hamiltonian at time t, and $E_n(t)$ is its corresponding eigenvalue. Now let us have a parametric

description of the Hamiltonian by introducing a set of variables $\mathbf{R}(t) = (r_1(t), r_2(t), r_3(t), ..., r_n(t))$ that implicitly depend on time. These parameters can be the diagonal entries of H, the off-diagonal terms, or even a phase between matrix elements. With this parametrization, we can now write

$$H(\mathbf{R})|n(\mathbf{R})\rangle = E_n(\mathbf{R})|n(\mathbf{R})\rangle \tag{2.4}$$

If we go to the parametric space defined by $(r_1, r_2, r_3, ..., r_n$, each coordinate here represents a unique configuration of our Hamiltonian. $\mathbf{R}(t)$ traces a curve in this space as time passes. As it moves, it also varies H at each point. The TDSE in this parametric picture becomes:

$$i\hbar\frac{\partial|\psi(\mathbf{R}(t))\rangle}{\partial t} = H(\mathbf{R}(t))|\psi(\mathbf{R}(t))\rangle \tag{2.5}$$

Now that we know our system's state at any arbitrary parameter point, can we say the phase remains unchanged in this time evolution? No. If we ignore time dependence in H for a moment, we still see the global phase of eigenstate changes in our system as $e^{\frac{-iEt}{\hbar}}$. So we have to include a global phase to describe our instantaneous eigenstate as:

$$|\psi(t)\rangle = e^{-i\theta(t)}|n(\mathbf{R}(t)\rangle \tag{2.6}$$

Multiplying Eq. 2.5 with the bra $\langle n(\mathbf{R}(t))|$ and using Eq 2.6, we get the relation of this global phase as:

$$\theta(t) = \frac{1}{\hbar}\int_0^t E_n(\mathbf{R}(t'))dt' - i\int_0^t \langle n(\mathbf{R}(t'))|\frac{d}{dt'}|n(\mathbf{R}(t'))\rangle dt' \tag{2.7}$$

The first term represents the global phase that trivially appears as an outcome of TDSE. However, another term appears because we move around the parametric space with time. The negative of this phase is called the Berry phase. In other words, the Berry phase

$$\begin{aligned}\gamma_n &= i\int_0^t \langle n\left(\mathbf{R}\left(t'\right)\right)|\nabla_{\mathbf{R}}|\, n\left(\mathbf{R}\left(t'\right)\right)\rangle \frac{d\mathbf{R}}{dt'}dt' \\ &= i\int_{\mathbf{R}_0}^{\mathbf{R}_t} \langle n(\mathbf{R})\,|\nabla_{\mathbf{R}}|\, n(\mathbf{R})\rangle\, d\mathbf{R} \\ &= \int_{\mathbf{R}_0}^{\mathbf{R}_t} \mathbf{A}_n(\mathbf{R})d\mathbf{R}\end{aligned}$$

where we have defined a new term called Berry potential as:

$$A_n(\mathbf{R}) = i\langle n(\mathbf{R})|\nabla_{\mathbf{R}}|n(\mathbf{R})\rangle \tag{2.8}$$

This is the phase that distinguishes two physical systems on the grounds of topology. When we have a closed curve in the parametric space, the surface integral over the Berry curvature is defined as

$$\Omega_n = \nabla_R \times A_n(R) \tag{2.9}$$

will give a non-zero phase for systems with discontinuity in the parameter space. We will see this in detail as we explore the eigenspectrum of our SSH model.

2.3 The Su-Schrieffer–Heeger (SSH) model

The SSH model is a toy model that gives a good intuition and flavor of the concepts of topology seen in a physical system. These basic ideas can be generalized in higher dimensional lattice models to understand phenomena such as edge conduction in a bulk insulating material.

The SSH model is a tight-binding model that simulates a dimerized lattice chain with an imbalance in the hopping parameter. As shown in Fig. 2.2, a dimerized lattice has two sites, A and B, in a primitive cell. This two-

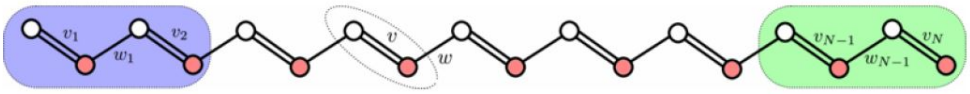

Figure 2.2: A dimerized lattice chain in 1D that shows imbalance in hopping within its cell v, and between cells w Site A is shown in white color while site B is shown in orange color.

site primitive cell can be translated by units of lattice constant to define a complete 1D chain. Hopping within a primitive cell that moves particle from site A to B has a hopping strength v, whereas hopping to its next cell has a different hopping strength w. In second quantized formalism, the Hamiltonian of a 1D SSH model by just considering hopping terms can be given as:

$$\hat{H} = -\sum_i v\left(\hat{a}_i^\dagger \hat{b}_i + \hat{b}_i^\dagger \hat{a}_i\right) + w\left(\hat{b}_i^\dagger \hat{a}_{i+1} + \hat{a}_{i+1}^\dagger \hat{a}_i\right) \tag{2.10}$$

2.3.1 Eigenvalues and eigenstates

Our goal is to obtain the eigenspectrum of this tight-binding model. To find that, we first make some simplifications to make our calculations look neat. First, we assume we have N primitive cells and, correspondingly, $2N$ sites in our 1D lattice. We assume periodic boundary conditions (PBC) and also assume we have unit spacing between lattice cells. With all these assumptions set to exploit the translational invariance in our system, we perform the Fourier transform and go to the momentum space by using

$$\hat{a}_j = \frac{1}{\sqrt{N}} \sum_{k \in FBZ} e^{ikj} \hat{f}_k,$$
$$\hat{b}_j = \frac{1}{\sqrt{N}} \sum_{k \in FBZ} e^{ikj} \hat{g}_k$$

After eating up some Kronecker deltas, we get a neat simplified Hamiltonian in the momentum space as:

$$H = -\sum_k (v + ie^{ik}w)\hat{f}_k^\dagger \hat{g}_k + (v + ie^{-ik}w)\hat{g}_k^\dagger \hat{f}_k \tag{2.11}$$

We see that each momentum block is coupled only to operators in its cell and not to other values of k. So, if we diagonalize their corresponding 2×2 momentum blocks, we have solved for all the energy eigenvalues and eigenstates. We represent a momentum block H_k as

$$H_k = \begin{pmatrix} \hat{f}_k^\dagger & \hat{g}_k^\dagger \end{pmatrix} \begin{pmatrix} 0 & v + ie^{ik}w \\ v + ie^{-ik}w & 0 \end{pmatrix} \begin{pmatrix} \hat{f}_k \\ \hat{g}_k \end{pmatrix}$$

(2.12)

We can get the total Hamiltonian by summing over the matrix blocks $H = \sum_k H_k$. The eigenvalues and eigenstates of each momentum block can be calculated as

$$E_\pm(k) = \pm\sqrt{v^2 + w^2 + 2vwcos(k)} \tag{2.13}$$

$$|\pm k\rangle = \begin{pmatrix} \pm e^{-i\phi(k)} \\ 1 \end{pmatrix} \tag{2.14}$$

where

$$\phi(k) = tan^{-1}\left(\frac{wsin(k)}{v + wcos(k)}\right) \tag{2.15}$$

Fig. 2.3 shows the band structure of our system within the FBZ. We see from Eq. 2.13 that the minimum of E_+ and the maximum of E_- do not always coincide. The band gap between those two levels is

$$\begin{aligned} E_g &= min(E_+) - max(E_-) \\ &= |v - w| - (-|v - w|) \\ &= 2|v - w| = 2\Delta \end{aligned}$$

Hence, our 1D lattice exhibits the behavior of an insulator for $v \neq w$.

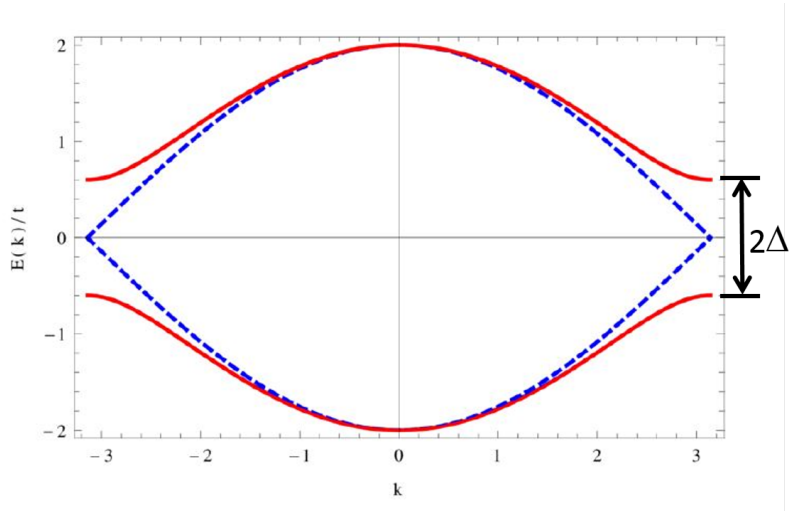

Figure 2.3: The energy eigenspectrum of our 1D SSH model with PBC. Dashed ones represent the band when $v = w$, and solid red one represents the band when $v \neq w$.

This band diagram also tells another exciting story. The energy spectrum of a dimerized chain is lower in energy than that of a uniform one if the energy band is half-filled. Our 1D chain is in an unstable energy configuration when it has equal hopping between sites. So 1D chains tend to redistribute their electron cloud distribution, creating a hopping imbalance between neighboring lattice sites. This phenomenon is known as Peierl's instability. It is seen in polyacetylene molecules where such an imbalance in hopping exists despite having bond conjugation and resonance throughout the molecule[20].

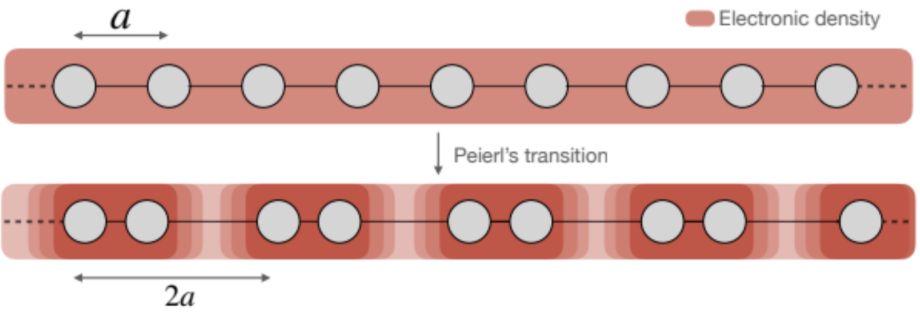

Figure 2.4: A 1D lattice that undergoes a Peierl's transition to stabilize itself. The resultant molecule becomes dimerized.

2.3.2 Topology and winding number

Since our eigenvalues are symmetric on the interchange between v and w, we might conclude that these two are equivalent systems. We can always redefine our primitive lattice cell by shifting it by one lattice site and say this physically correspond to $v \to w$ and $w \to v$. However, we will be throwing away an essential property of our system if we conclude their equivalence by looking at the eigenspectrum and ignoring their corresponding momentum states. It is when we analyze the eigenstates that we realize the topology enters into our system!

Let us go back to the $H(k)$ we had derived earlier in Eq. 2.12. This 2×2 matrix can be decomposed into components of the Pauli matrices $\{\sigma_i\}$ as:

$$\begin{aligned} H(k) &= \begin{pmatrix} 0 & v + ie^{ik}w \\ v + ie^{-ik}w & 0 \end{pmatrix} \\ &= (v + wcos(k)) \begin{pmatrix} 0 & 1 \\ 1 & 0 \end{pmatrix} + wsin(k) \begin{pmatrix} 0 & i \\ -i & 0 \end{pmatrix} + 0 \begin{pmatrix} 1 & 0 \\ 0 & -1 \end{pmatrix} \\ &= \bar{h}(k).\bar{\sigma} \end{aligned}$$

where

$$\bar{h}(k) = h_x(k)\hat{x} + h_y(k)\hat{y} = (v + wcos(k))\hat{x} + wsin(k)\hat{y} \tag{2.16}$$

If we use a small amount of high school geometry, we can trace $\bar{h}(k)$ as a circle with radius $|w|$ centered at $|v|$ in the $h_x - h_y$ plane. As we vary k within the FBZ, we get $\bar{h}(k)$ as the locus of points that move around this circle. Fig. 2.5 shows this geometric visualization. So, our momentum states have the topology of a ring in our parametric space.

Now, we go back to the adiabatic theorem and slowly vary our Hamiltonian to move around all the momentum vectors in the FBZ. Our parameter

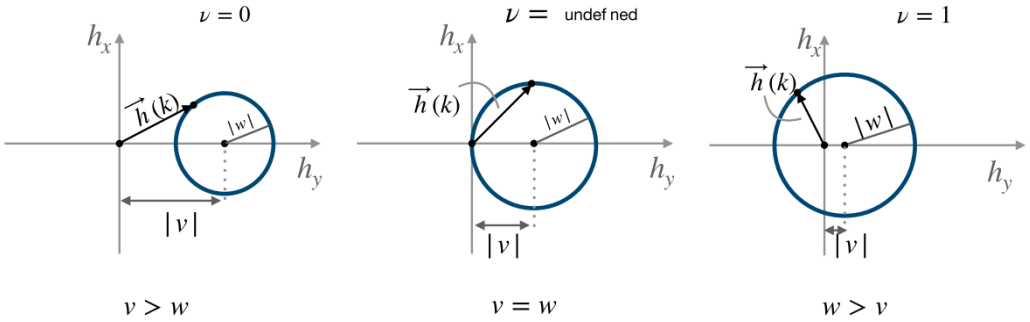

Figure 2.5: Trajectories followed by $\bar{h}(k)$ as we move around the FBZ. The three cases when $v > w$, $v = w$, and $v < w$ are shown. We get a non-zero winding number when our circle crosses the origin[19].

becomes the momentum k, and the corresponding Berry potential we have for the eigenstates defined by this parameter, using Eq. 2.8 becomes:

$$A_{\pm}(k) = i \left\langle \pm k \left| \frac{d}{dk} \right| \pm k \right\rangle \tag{2.17}$$

Substituting for $|\pm k\rangle$ from Eq. 2.14 in 2.17, we get:

$$A_{\pm}(k) = -\frac{1}{2}\frac{d\phi(k)}{dk} \tag{2.18}$$

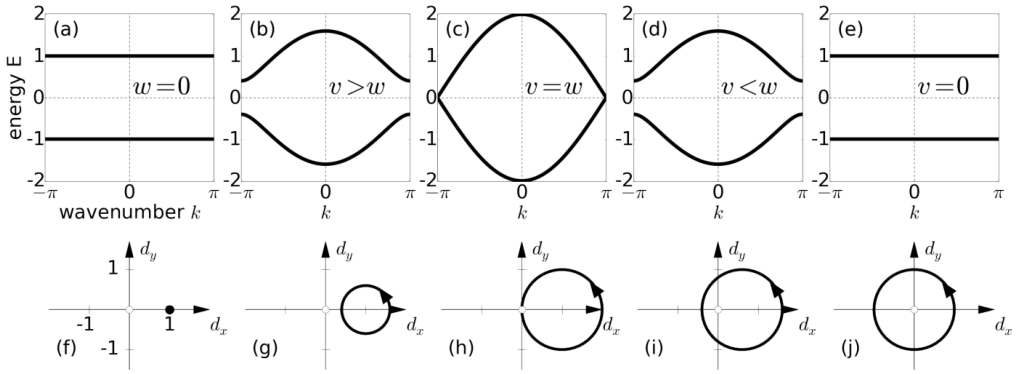

Figure 2.6: The energy spectrum (a)-(e) and their corresponding topology in the phase space (f)-(j) obtained for various cases of v and w. We see that there is a distinction in the topology of these momentum states even though the eigenvalues seem identical[18].

If we perform the surface integration of our Berry curvature, or equivalently the loop integration of the Berry potential along the perimeter of the surface, we get:

$$\begin{aligned}\oint A_{\pm}(k)dk &= \oint -\frac{1}{2}\frac{d\phi(k)}{dk}dk \\ &= -\frac{1}{2}\oint d\phi \\ &= \begin{cases} 0 & \text{if } v > w \\ \text{undefined} & \text{if } v = w \\ -\pi & \text{if } v < w \end{cases}\end{aligned}$$

On returning to the same state after going around our FBZ, we end up with a phase of $\gamma_k = \pi$ for one system while we get nothing in the other case. This shows that these two systems are, in reality, *not* equivalent, and they are distinguished by the topological features defined by the Berry curvature. We can go one step further and get an excellent correspondence to the Gauss-Bonnet theorem by defining the winding number or Chern's number

$$g = -\frac{1}{\pi}\oint A_{\pm}(k)dk \tag{2.19}$$

This number now tells us how many times we go around the origin as we traverse through the momentum states in our FBZ and distinguish our system based on this topological invariant.

2.3.3 Edge states in a finite SSH model

So far, we have seen how topology can bring inherent distinction between two systems that might look identical superficially. Now we look at one direct physical outcome of this topological formulation. However, to see this, we must go out of our comfort zone of living in a world that is set simply by periodic boundary conditions. Now we consider an SSH model with open-boundary conditions (OBC) and solve for its eigenspectrum. We first look at the intuitive behavior of our system at two extreme regimes of v and w.

Fig. 2.7 shows the SSH model in two extreme scenarios. When we have extensive intracell hopping, as in Fig. 2.7(a), our system turns into N-isolated dimers with eigenvalues corresponding to the two eigenvalues of a single dimer unit, so we have N-fold degeneracy in each of these eigenstates. However, we see an exciting outcome if we look at Fig. 2.7(b). There are $N-1$ degenerate dimers in bulk and two edge states that exist isolated from the

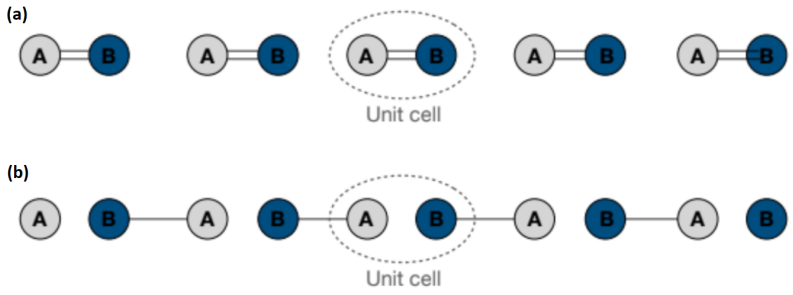

Figure 2.7: Two extreme cases of our SSH model. (a) shows the scenario when intracell hopping is finite, and intercell hopping is zero. (b) shows the case when intracell hopping is zero, and intercell hopping is finite.

bulk. These edge states have zero energy since they neither overlap orbitals to get stability through hopping nor have self energies. So we have *two* edge states and $N-1$ bulk dimer states. Now we shall see this phenomenon more precisely by numerically solving the tight-binding model with OBC (we can no longer afford the luxury of using translational invariance, and hence our only hope is a numerical solution).

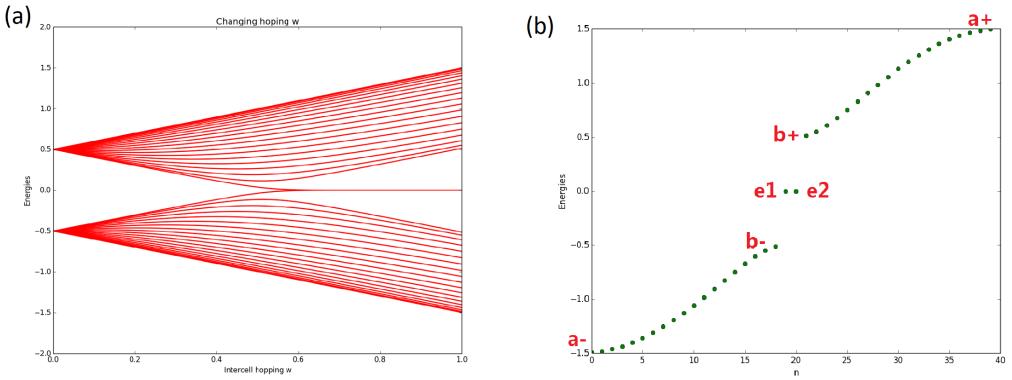

Figure 2.8: Analysis of eigenspectrum of a 40-site SSH model with OBC. (a) shows the eigenspectrum of our SSH model as we vary w from 0 to 1 by keeping $v = 0.5$. We see the introduction of two energy states corresponding to the edge states as we cross the $v = w$ regime. (b) shows the discrete energy spectrum of our model at $v = 0.5, w = 1$.

Fig. 2.8(a) describes our system as it transitions from one regime to the other. At $w = 0$, we have two N-degenerate eigenstates corresponding to

the bulk dimers we see in the absence of intercell hopping. As we increase w, the band gap between the two bands comes closer, and as we reach the regime where $w = v$, we have the introduction of edge states. These states remain even after we increase w more than v and, in turn, increase the band gap. These edge states are seen in our system when our system undergoes a topological phase transition from a trivial insulator, $g = 0$, to a topological insulator, $g = 1$, as we had seen earlier in Eq. 2.19. To ensure these states correspond to the edge state, we take the case when we are in a topological insulator state (i.e.), $v = 0.5$, $w = 1$, and plot its energy spectrum in the FBZ (Fig. 2.8(b)). Now we plot the spatial distribution of the eigenstates at the lowest valence band (a-), highest valence band (b-), edge states (e1 and e2), lowest conduction band (b+), and highest conduction band (a+). Fig. 2.9 shows the plots

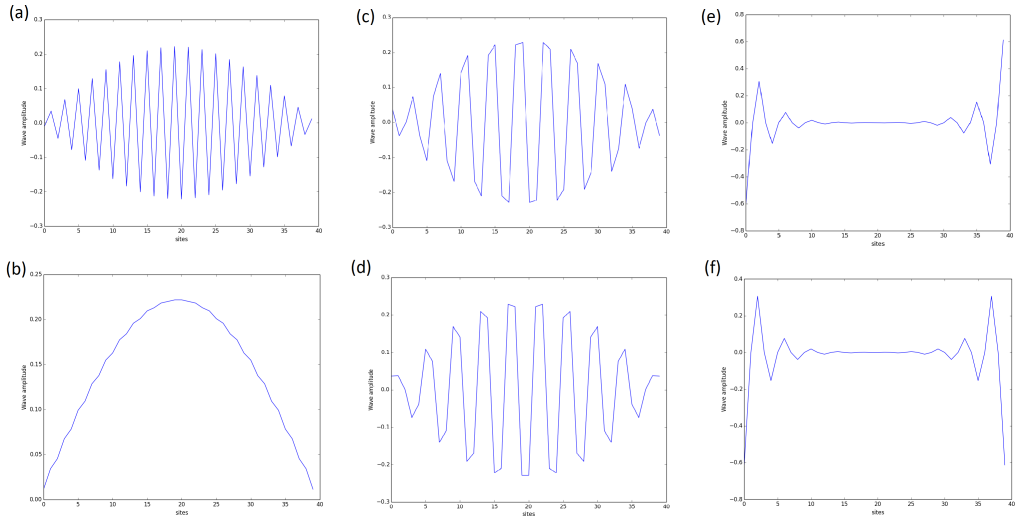

Figure 2.9: Eigenstates of our SSH model in the topological insulator regime. (a) represents a-, (b) a+, (c) b-, (d) b+, (e) e1, (f) e2.

(a) and (c) show the valence band's lowest and highest energy eigenstate. They both have good bulk distribution. The same goes for the lowest and highest energy eigenstates of the conduction band in (d) and (b). However, if we look at (e) and (f), both these states have exponentially decaying spatial distribution as they go into the bulk, meaning they are localized in the edges. These are the edge states that the topology of our system has introduced! It is no coincidence that they appeared when we moved from $w < v$ to $w > v$. This is a direct outcome of the topology of our material, and this is an example of Bulk-boundary correspondence where we look at the properties

of the bulk, calculate its topological invariants, and assert whether these edge states can exist in our system.

2.4 Discrete-time quantum walks

Before introducing continuous-time quantum walk, we shall see a brief overview of a discrete-time quantum walk as it gives some motivation to appreciate physical processes that involve quantum walks. DTQW is an algorithm (more than a physical process) where a random decision is made with the help of a unitary operator known as the "Quantum coin", and based on it the walker propagates across space. In general, we consider a space of $\mathcal{H}_p = |n\rangle$, n being an integer, as the space where our walker walks. Now, this walker is carrying a tag of possible outcomes as he walks. If it is a fermion, it can be the spin of the fermion that has the outcome of "up" or "down". This decision space $\mathcal{H}_c = |0\rangle, |1\rangle$ is therefore a space of two states. If the spin is up, our particle walks left, and if down, it moves right. Thus, the space of our particle $\mathcal{H}$ that we use to perform QW is the combined space of spin and integer space. The quantum coin acts only on the spin space, and the propagation $\hat{S}$ only happens in integer space depending on the state of the spin. Formally writing the above, we have:

$$\mathcal{H} = \mathcal{H}_c \otimes \mathcal{H}_p \tag{2.20}$$

$$\hat{S}|0, n\rangle = |0, n+1\rangle$$
$$\hat{S}|1, n\rangle = |1, n-1\rangle$$

Thus, summing over all sites, our propagation operator becomes:

$$\hat{S} = |0\rangle\langle 0| \otimes \sum_{n=-\infty}^{\infty} |n+1\rangle\langle n| + |1\rangle\langle 1| \otimes \sum_{n=-\infty}^{\infty} |n-1\rangle\langle n| \tag{2.21}$$

Now we are left with defining the quantum coin to perform a quantum walk. In principle, any unitary operator in $\mathcal{H}_c$ should do the job. However, it must be a unitary operator since the particle must preserve the norm (and thus the probability axioms), as it walks. Each unitary operator will produce its own unique QW in $\mathcal{H}_p$. However, one of the most commonly used coins is the Hadamard coin defined as:

$$H = \frac{1}{\sqrt{2}} \begin{bmatrix} 1 & 1 \\ 1 & -1 \end{bmatrix} \tag{2.22}$$

So at each step of the walk, we first flip the coin and then act the propagator on it to do the walk.

$$U = \hat{S}.(H \otimes I) \tag{2.23}$$

So, the state of our particle at time t is given by:

$$|\psi(t)\rangle = U^t|\psi\rangle \tag{2.24}$$

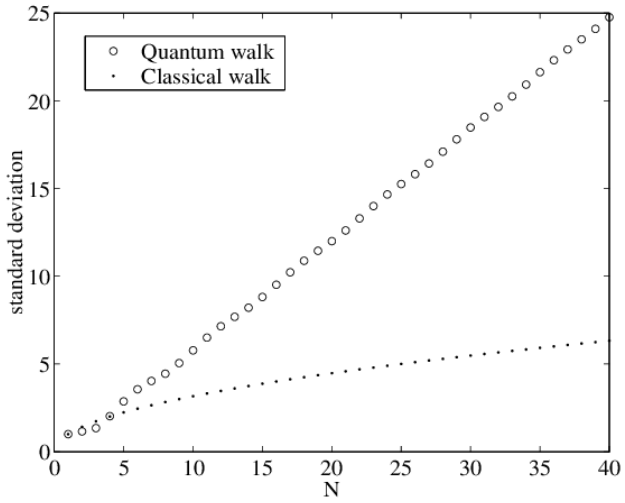

Figure 2.10: σ of Classical and Quantum walks vs iterations[22].

Even though this algorithm is pretty straightforward, it has interesting properties. The walk is very different from the classical walk as at each step, the fermion is in a vague superposition of both up and down spin and hence it propagates faster to the edges than the classical walk where superposition doesn't make sense. The quantification of how "fast" the particle propagates in the lattice is defined by the standard deviation σ. $\sigma_{clasical} \sim \sqrt{t}$ whereas $\sigma_{quantum} \sim t$. Fig. 2.10 shows the comparison of it. The probability distribution of our walk is extremely sensitive to the initial configuration of our spin even if the initial position, the quantum coin, and everything else remain unchanged. Fig. 2.11 shows the effect of different initial spin configurations. Another feature that doesn't exist in CW.

2.5 Classical walks and its quantization

Physical quantum walks are defined on a directed graph where the vertices play the role of the states our walker can be in, and the directed edges play

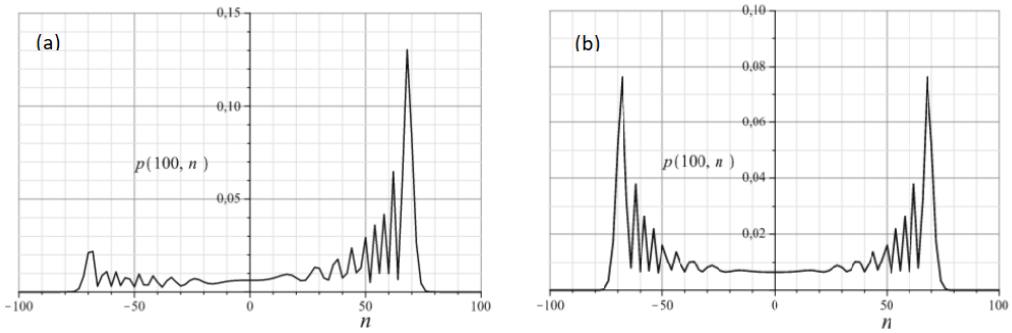

Figure 2.11: Probability distribution of DTQW with different initial spin configurations[23]. (a) QW with initial spin $|0\rangle$. (b) QW with initial spin $\frac{1}{\sqrt{2}}(|0\rangle - i|1\rangle)$.

the role of going from one state to the other. Now in this system, we introduce stochasticity (i,e) the walker takes a decision at each step of the walk and proceeds to the next state depending on the decision he takes. We consider one such stochastic process called the Markov process where the stochasticity is choosing one of the adjacent vertices with a probability corresponding to the weight of the directed edge.

2.5.1 Classical Markov process

A Markov process is a stochastic process that has two main underlying properties:

1. The decision of going to $n+1th$ state from nth state only depends on the decision taken at nth step and *not* on the decisions that he might've taken at previous states.

2. The next state is determined by randomly choosing a directed edge originating from his current state with a probability equal to the weight of the corresponding edge.

Fig. 2.12 shows a Markov process with three states and directed edges denoting transition between them. We can describe the state of the walker at time t by a state vector with its ith coefficient denoting the probability of being in the ith state.

$$\bar{p}(t) = \begin{bmatrix} p_1(t) \\ p_2(t) \\ \dots \\ p_n(t) \end{bmatrix} \tag{2.25}$$

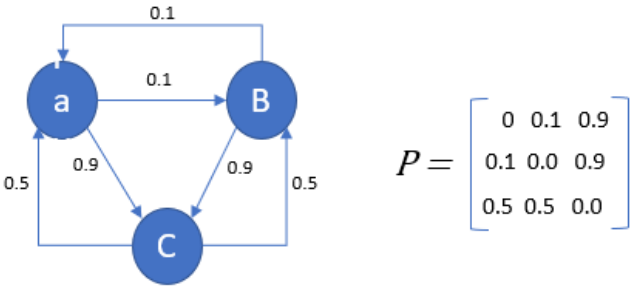

Figure 2.12: An example of a Markov process with its corresponding transition matrix.

Here t can be in steps, or continuous. We start with discrete t and then proceed to its continuum limit. From the second property of Markov processes, we can say the probability of reaching state i at time t is the sum over all possible state j it could've been in time $t-1$ and then jumping to state i with probability T_{ij}. This can be written as:

$$p_i(t) = \sum_j T_{ij} p_j(t-1)$$

So, if we construct a transition matrix T with its coefficient T_{ij} denoting the probability of going from state j to i, we have the recursive stochastic equation:

$$\bar{p}(t+1) = M.\bar{p}(t) \tag{2.26}$$

We observe that the $t+1$th step only depends on its decision in the previous step and not on its far past decisions and so, retains the conditions of a Markov process. Now that we have written the entire process as a linear equation, we can write the state at time t in terms of the state at $t=0$ by using the properties of linear equations:

$$\bar{p}(t) = M^t.\bar{p}(0) \tag{2.27}$$

There are much more interesting analyses of a classical Markov process such as finding the stationary state that the walker will be after a very large number of steps by finding eigenvalues and eigenstates of T. But the provided background suffices to understand the continuum limit of classical walks and quantizing it to obtain the CTQW equations that we will be using in our simulation of QW of bosons.

2.5.2 Continuous classical walks and their quantization

In the system we wish to study, we have an optical lattice in which bosonic particles perform a walk by hopping from one site to another. Since our lattice has an inherent property of symmetry, the lattice site i is identical to sites $i+1$, $i-1$, $i+2$, and so on. Hence, we can use translational invariance to say the hopping rate from a site i to any of its adjacent sites must be equal. Let this hopping rate be γ. Now consider an infinitesimal time step ϵ. The probability of going to one of the adjacent sites is $p_{ij} = \epsilon\gamma$. If our site j has d_j neighbors then, our boson has the probability of $1 - d_j\epsilon\gamma$ of being in site j. Thus, our infinitesimal transition matrix $T(\epsilon)$ is given as:

$$T_{ij}(\epsilon) = \begin{cases} 1 - d_j\epsilon\gamma & \text{if } i = j \\ \epsilon\gamma & \text{if } i \neq j \text{ and adjacent} \\ 0 & \text{if } i \neq j \text{ and not adjacent} \end{cases} \tag{2.28}$$

With the above definition, we use the properties of the Markov process to write:

$$\begin{aligned} M_{ij}(t+\epsilon) &= \sum_k M_{ik}(t)M_{kj}(\epsilon) \\ &= M_{ij}(t)M_{jj}(\epsilon) + \sum_{k\neq j} M_{ik}(t)M_{kj}(\epsilon) \\ &= M_{ij}(t) - \epsilon\gamma d_j M_{ij}(t) - \epsilon\gamma \sum_{<k>} (-1)M_{ik}(t) \end{aligned} \tag{2.29}$$

where $< k >$ considers only the adjacent terms to i. We define a generating matrix H to simplify the above expression and rewrite it in terms of it:

$$H_{ij}(\epsilon) = \begin{cases} d_j & \text{if } i = j \\ -1 & \text{if } i \neq j \text{ and adjacent} \\ 0 & \text{if } i \neq j \text{ and not adjacent} \end{cases} \tag{2.30}$$

We note that H is the same as the laplacian of a graph with uniform hopping to adjacent sites. Eq. 2.29 in terms of H simplifies to:

$$\begin{aligned} M_{ij}(t+\epsilon) &= M_{ij}(t) - \epsilon\gamma \sum_k H_{ik}.M_{kj}(t) \\ \implies \frac{M_{ij}(t+\epsilon) - M_{ij}(t)}{\epsilon} &= -\gamma \sum_k H_{ik}.M_{kj}(t) \end{aligned}$$

Thus, we arrive at the Master equation for our Markov process:

$$\frac{d}{dt}M(t) = -\gamma H.M(t) \tag{2.31}$$

$$\frac{d}{dt}\bar{p}(t) = -\gamma H.\bar{p}(0) \tag{2.32}$$

For an initial state with the initial condition $M_{ij}(t=0) = \delta_{ij}$, this yields:

$$M(t) = e^{-\gamma Ht} \tag{2.33}$$

$$\bar{p}(t) = e^{-\gamma Ht}\bar{p}(0) \tag{2.34}$$

If we look at $M(t)$ in its eigenbasis, it has a diagonal form with its entries as an eigenvalue of the form $\sim e^{-\gamma\lambda_i t}$. Thus, in a classical Markov process, our walker's probabilities exponentially decay to its stationary eigenstate or oscillate between states depending on whether λ_i is real or imaginary respectively.

Quantising Eq. 2.32 demands us to replace $\frac{d}{dt}$ operator with $i\hbar\frac{d}{dt}$, consider γH as our Hamiltonian, and replace the probability vector by a state vector in the space of lattice sites $|N\rangle$. Assuming $\hbar = 1$, Eq. 2.13 takes the form of Schrodinger equation on quantizing:

$$i\frac{d}{dt}|\psi(t)\rangle = \hat{H}|\psi(t)\rangle \tag{2.35}$$

Thus, our unitary time propagator analogous to $M(t)$ in Eq. 2.33 becomes:

$$\hat{U}(t) = e^{-i\hat{H}t} \tag{2.36}$$

The quantum analog of Eq. 2.34 is given by:

$$|\psi(t)\rangle = e^{-i\hat{H}t}|\psi(0)\rangle \tag{2.37}$$

After time t, the probability of our boson being in state n is given by:

$$p_n(t) = |\langle n|\psi(t)\rangle|^2 = |c_n(t)|^2 \tag{2.38}$$

Eq. 2.35 can be solved numerically by defining the appropriate H where the diagonal terms define the potential energy of being in its site, and the off-diagonal terms are the hopping energy of going from one site to another. However, in the problem of QW by a single boson in a 1D lattice with hopping between the nearest sites, we can exactly solve the equation to get

the analytical expression of state after time t. The 1D Hamiltonian is defined as:

$$H = \begin{cases} 2\gamma & \text{if } i = j \\ -\gamma & \text{if } i \neq j \text{ and adjacent} \\ 0 & \text{if } i \neq j \text{ and not adjacent} \end{cases} \quad (2.39)$$

If our particle is in the state $|n\rangle$, then:

$$H|n\rangle = 2\gamma|n\rangle - \gamma|n+1\rangle - \gamma|n-1\rangle$$

We can write the k power of H acting on $|0\rangle$ as:

$$H^k|0\rangle = \gamma^k \sum_{n=-k}^{k} (-1)^k \binom{2k}{k-n} |n\rangle \quad (2.40)$$

where $\binom{2k}{k-n}$ represents the possible ways to reach state $|n\rangle$ after k steps. So, using Eq. 2.37, and assuming our particle starts from $|0\rangle$, we get:

$$\begin{aligned} |\psi(t)\rangle &= e^{-iHt}|0\rangle \\ &= \sum_{k=0}^{\infty} \frac{(-it)^k}{k!} H^k|0\rangle \\ &= \sum_{k=0}^{\infty} \frac{(-it)^k}{k!} \gamma^k \sum_{n=-k}^{k} (-1)^k \binom{2k}{k-n} |n\rangle \\ &= \sum_{k=0}^{\infty} \sum_{n=-k}^{k} \frac{(-i\gamma t)^k}{k!} e^{i|n|\pi} \binom{2k}{k-n} |n\rangle \end{aligned}$$

Summing n from $-k$ to k over k from 0 to ∞ is the same as summing n from -∞ to ∞ over k from $|n|$ to ∞. So we invert the sum to get:

$$|\psi(t)\rangle = \sum_{n=-\infty}^{\infty} \sum_{k=|n|}^{\infty} \frac{(-i\gamma t)^k}{k!} e^{i|n|\pi} \binom{2k}{k-n} |n\rangle \quad (2.41)$$

Now using the identity of the Bessels function:

$$e^{2ix} J_{|n|}(2x) = e^{i\frac{i}{2}|n|} \sum_{k=|n|}^{\infty} \frac{(-ix)^k}{k!} \binom{2k}{k-n} \quad (2.42)$$

we eliminate the sum over k in Eq. 2.22 to obtain:

$$|\psi(t)\rangle = \sum_{n=-\infty}^{\infty} e^{i\frac{\pi}{2}|n| - 2i\gamma t} J_{|n|}(2\gamma t)|n\rangle \quad (2.43)$$

So the probability of being in state n is:

$$p_n(t) = |c_n(t)|^2 = |J_{|n|}(2\gamma t)|^2 \tag{2.44}$$

The probability is symmetric about n. So the boson propagates identically

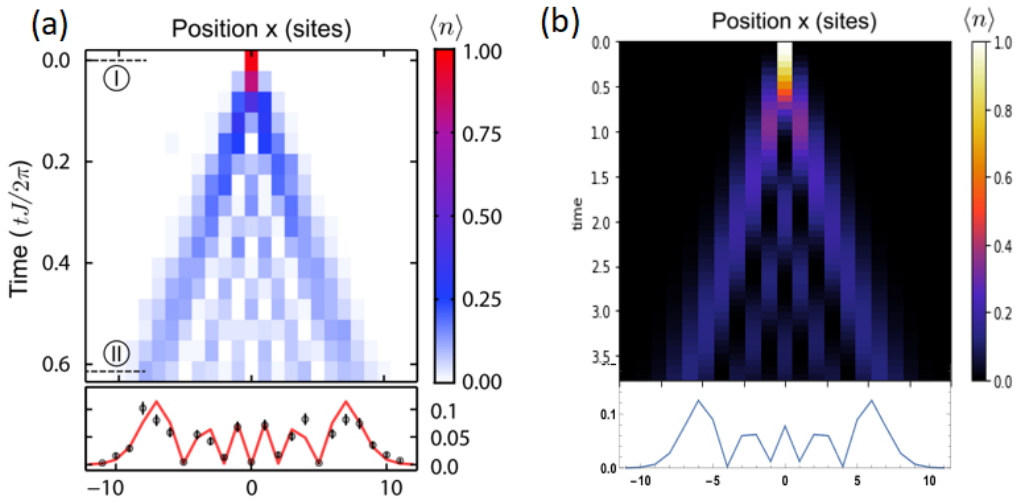

Figure 2.13: Experimental verification of the analytical probability distribution derived for a single particle CTQW. (a) Experimental result of a single Boson CTQW[21]. (b)Numerical plot of Eq. 2.25 with $\gamma = 1$ and $t = 3.7$.

on both sides of the lattice. Eq. 2.44 is confirmed by the experimental result of one boson QW by *Preiss et.al* as shown in Fig. 2.13 (a).

Chapter 3

Results

We have already simulated a single particle SSH model and solved for its energy spectrum and edge states in section 2.3.3. We have also simulated a single particle quantum walk in section 2.5.2 and compared its results with the analytical formula. The story becomes complicated when we have interaction in our lattice. In that case, our SSH model in Eq. 2.10 gets modified to

$$\hat{H} = -\sum_i v\left(\hat{a}_i^\dagger \hat{b}_i + \hat{b}_i^\dagger \hat{a}_i\right) + w\left(\hat{b}_i^\dagger \hat{a}_{i+1} + \hat{a}_{i+1}^\dagger \hat{a}_i\right) + \frac{U}{2}(\hat{n}_{a_i}(\hat{n}_{a_i}-1) + \hat{n}_{b_i}(\hat{n}_{b_i}-1)) \tag{3.1}$$

Since we sum only over primitive cells, we need to explicitly include the interaction in each site of our primitive cell. $\hat{n}_{a_i}$ represents the number operator of site A of ith primitive cell, and similarly $\hat{n}_{b_i}$.

We use *quspin*[25] library to perform exact diagonalization and numerically solve the 1D SSH model with interaction existing between particles. We consider a finite chain lattice of 20-sites with two bosons that follow the quench dynamics defined by TDSE of Eq. 3.1. We first look at the case when we have no interaction and get the effect of topology we had predicted in section 2.3.3 for our two-particle system.

3.1 QW on the SSH model without particle interaction

Fig. 3.1 shows the QW of two bosons initialized at the center of our lattice. If we set equal hopping $v = w$, we get our good old single-particle quantum walk

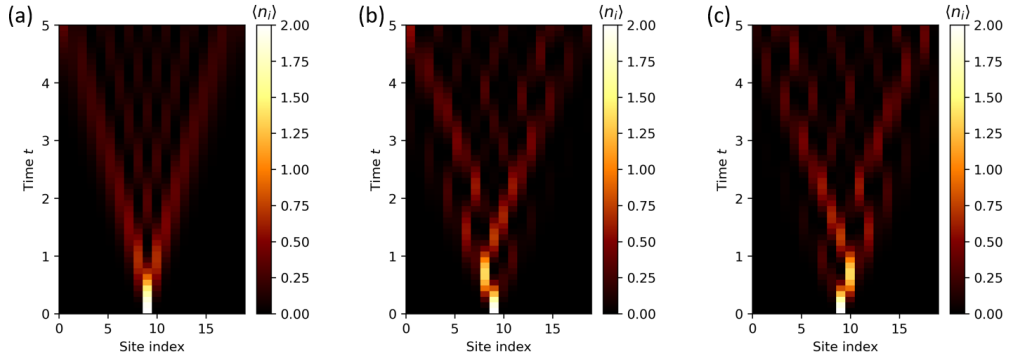

Figure 3.1: QW of our system with two bosons initialized at the center. (a) shows the case when $v = w = 1$, (b) shows when $v = 2, w = 1$, and (c) shows when $v = 1, w = 2$.

as seen in section 2.5.2, only now with two particles. This is because they are performing their independent quantum walk in the absence of interaction. If we have increased and decreased intracell hopping w.r.t intercell hopping such that $|v - w|$ remains the same in both, we get symmetric quantum walks as seen in Fig. 3.1 (b) and (c). This is expected since we effectively interchanged v and w in those diagrams, and now the particle that moved left initially will move oppositely, thus creating a walk that is the mirror image of the other. This is the bulk behavior of our system when we go to a topological system. Now to the edge behavior!

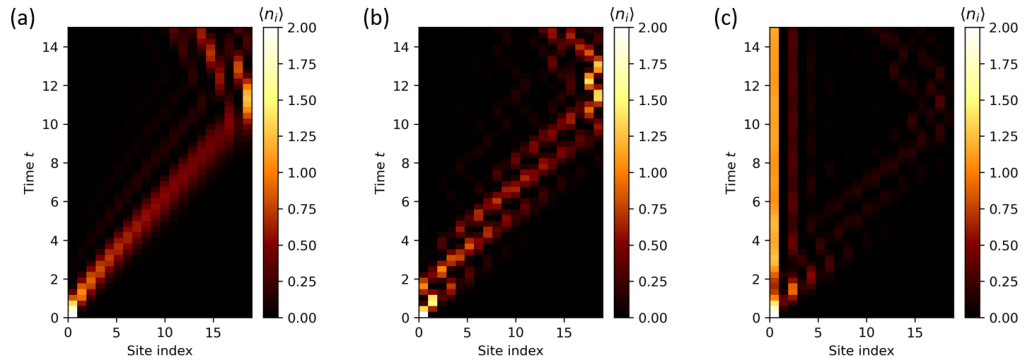

Figure 3.2: QW of our system with two bosons initialized at the left edge of our lattice. (a) shows the case when $v = w = 1$, (b) shows when $v = 2, w = 1$, and (c) shows when $v = 1, w = 2$.

Fig. 3.2 shows the same cases of v and w but now, with the two bosons initialized at the left edge of our lattice. When $v = w = 1$, we see two inde-

pendent QW superimposed such that our particle moves towards the right of our lattice and bounces back. If we introduce strong intracell hopping, we see our particle still moves towards the right, but now with more oscillations within a cell along with translation. However, we see entirely different dynamics when swapping v and w as in Fig. 3.1 (b) and (c). The particle gets localized chiefly at the left edge, with only a tiny fraction moving into the bulk with time. Here $v = w$ remains our topological transition point since we have yet to introduce interaction.

3.2 QW on the SSH model with particle interaction

The interacting system is difficult to solve analytically. Our interacting system does not need to show still a phase transition at $v = w$ like our non-interacting system. This is why we see topological states' effects getting erased as we increase interaction strength. This is illustrated in Fig. 3.3.

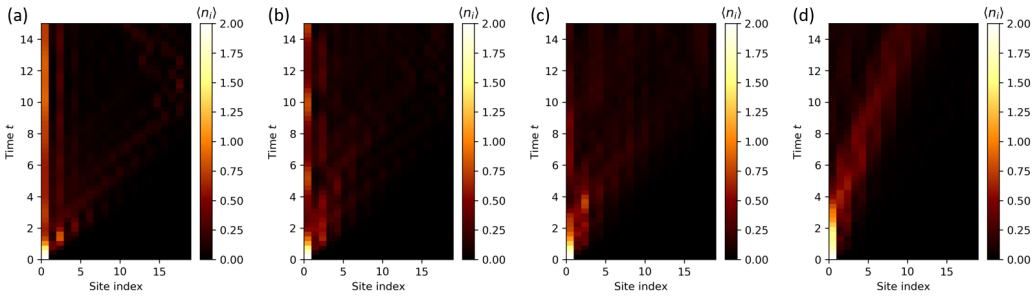

Figure 3.3: Loss of edge states when we introduce interaction in our system. With two bosons initialized at the edges, (a) shows the case when $U = 1$, (b) $U = 2$, (c) $U = 3$, and (d) $U = 5$.

As we increase the particle interaction, our edge state slowly seeps into the bulk. After a decent amount of interaction potential, the edge localization completely disappears, and the two-particle becomes a repulsively bound pair. Using bulk-boundary correspondence, the topology of our system has changed, due to which we lose the edge states that existed without interaction. Hence, interaction has the power to change the topology of our system!

Now to address how our boson pair becomes a repulsively bound particle, we go to Fig. 3.4. Repulsively bound pair is formed in a bosonic system

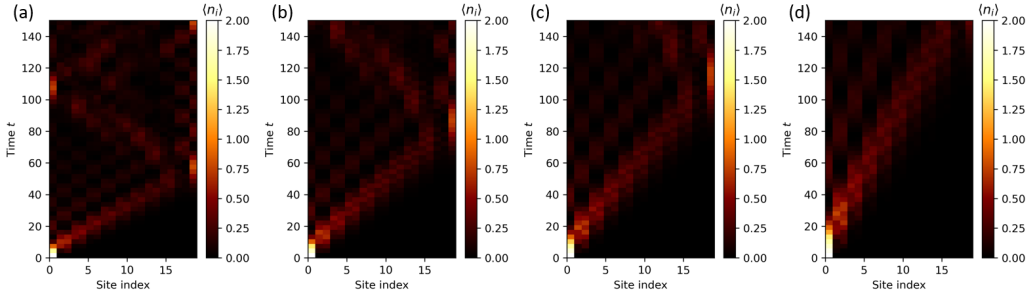

Figure 3.4: Formation of repulsively bound pairs for large U. (a) shows the QW of two bosons for $U = 10$, (b) $U = 15$, (c) $U = 20$, (d) $U = 30$. Note that the time scale is larger than the QW in Fig. 3.2.

when we introduce significant interaction between bosons. In our case, where bosons tend to repel each other when they occupy the same site, they become unstable when initialized at the same site. So they try to spread away from each other in such a situation. However, suppose we tip off the hopping by adding an immense on-site interaction potential. In that case, the particle becomes extremely unstable, but it cannot escape because the relative hopping term is insignificant. So, our bosonic pair continues to remain and behave like a bound pair, despite being repulsive. Experimenalists have realized this phenomenon on optical lattices with bosonic atoms[26]. In Fig. 3.4, we see the regime when the interaction has increased to values that create repulsively bound pairs, and our system performs a QW that is very similar to a free particle QW as in Fig. 3.2 (a). The repulsively bound pair now bounces back and forth our lattice as if it were a single particle, but it does so very slowly, to be precise, about ten times in order slower than that performed by non-interacting bosons. As we increase U, the repulsively bound pair becomes slower in its movement as it takes longer, T, to reach the other edge. Fig. 3.4 (a)-(d) shows this effect. For $U = 10$, $T \approx 55$, for $U = 15$, $T \approx 80$, for $U = 20$, $T \approx 110$, and for $U = 30$, $T \approx 160$ (the particle went out of the time-scale for our image). This shows that the interaction term plays the effective role of hopping; only now, an increase in U leads to a decrease in the hopping strength of our repulsively bound pair.

Chapter 4

Summary and future plans

4.1 Summary

In this first half of my thesis, we have primarily devoted our time to the background concept study that is quintessential for proceeding in the direction of topology effects in a condensed matter system. We have studied the theory of adiabatic processes and the Berry phase, Berry potential, and Berry curvature that comes as an outcome of geometric traversal in a parametric description of our Hamiltonian dynamics. We then connected with the mathematical concepts of topology and showed how they are introduced in physical systems. To apply these concepts in a toy model that can show topology effects, we solved the 1D SSH model analytically and plotted its eigenspectrum for both periodic and open boundary conditions. we have then shown how the momentum states have a topological invariant by exhibiting a similar winding effect as we traverse through the FBZ of our SSH model. we have also shown the two topological phases of our system and how edge states appear in one of them.

After finding the point when our 1D SSH model exhibits a topological phase transition, we proceeded to simulate the dynamics of this system with the help of continuous-time quantum walk formulation. We have briefly seen discrete-time quantum walk before diving into continuous Markov processes that lead us to the formulation of CTQW. With Schrodinger's equation definition of a quantum walk, we simulated it on a 20-site lattice with two bosons performing the quantum walk. We have used *quspin* library to get the time dynamics of this system by the exact diagonalization method. With this, we have mapped the average occupation of each site with time and showed our system's quench dynamics (quantum walk) at various system conditions.

Without introducing interaction, we have first shown how we get back the behavior of a single particle SSH model by simulating two particles QW's bulk and edge dynamics for the three cases that correspond to a trivial insulator phase, phase transition point, and the topological insulator phase. Then on adding interaction, we showed that the topological properties of our system can get erased. we have also argued that interaction can change the topology of our band structure. Finally, we have also shown our system's formation of repulsively bound pairs.

4.2 Future plans

- We shall continue this project by quantifying the topological invariant that tells us about the topology of our material. We shall also try to find the phase transition point when interaction exists and the conditions when the edge states reappear in our system, even in the presence of interaction.

- Next, We shall try introducing disorder in our system and see if localization appears in our lattice. Localization of bosons on the introduction of quasi-periodicity in an optical lattice has already been shown theoretically[17]. We shall explore the effects of localization in the context of the topology of the SSH model.

- We also hope to write a quantum algorithm to implement continuous-time quantum walk on a quantum computer. We shall use the trotterisation formalism to implement the unitary evolution of my system defined by the Master's equation Eq. 2.35 in a system performing quantum walk. Time dynamics of a spin system have already been implemented on a quantum computer[27]. We shall try applying the Jordan-Wigner transformation to convert spin dynamics to an equivalent description of spinless fermions performing the unitary time evolution.

Acknowledgment

I am writing to express my gratitude to Prof. Tapan Mishra for letting me work on this project and introducing me to the active field of topology and physics. A big thanks to my senior, Ashirbad Padhan, for holding Gmeets and helping me with coding whenever needed. Thank you, Mrinal Kant Giri, for helping me with the theory of quantum walks, and Rajashri di for giving me all the materials to get my hands-on work on this project (and correcting my reports). Thanks to Biswajit and Soumya dada for teaching me quantum computation and DMRG. I am blessed to work with such a supportive group. Thanks to Prof. Andrew Mitchell from the University of Dublin for providing open access to detailed lectures on condensed matter physics on youtube that has helped me get an excellent introduction to tight-binding systems. Thanks to my parents for believing in me and motivating me to do research, and Dr. Pratap Kumar Sahoo for supporting me during my existential crisis and suggesting valuable tips to enjoy my time in academia. Finally, a big thanks to the Almighty (Yes, I am religious).

References

[1] U Dallmann. Three-dimensional vortex structures and vorticity topology (1988). Fluid Dyn. Res. 3 183

[2] Heil, Matthias Rosso, Jordan Hazel, Andrew Brøns, Morten. (2017). Topological fluid mechanics of the formation of the Kármán-vortex street. Journal of Fluid Mechanics. 812. 199-221. 10.1017/jfm.2016.792.

[3] Joseph Avron, Daniel Osadchy, Ruedi Seiler. A Topological Look at the Quantum Hall Effect. Physics Today 56, 8, 38 (2003); https://doi.org/10.1063/1.1611351

[4] The Nobel Prize in Physics 2016. NobelPrize.org. Nobel Prize Outreach AB 2022. https://www.nobelprize.org/prizes/physics/2016/summary/

[5] Liang Fu and C. L. Kane. Topological insulators with inversion symmetry. Phys. Rev. B 76, 045302 (2007)

[6] Nagaosa, N., Tokura, Y. Topological properties and dynamics of magnetic skyrmions. Nature Nanotech 8, 899–911 (2013). https://doi.org/10.1038/nnano.2013.243

[7] Raimund Varnhagen. Topology and fractional quantum Hall effect (1995). Nuclear Physics B, 443(3), 501-515. https://doi.org/10.1016/0550-3213(95)00143-G

[8] Sondhi, S. L., Karlhede, A., Kivelson, S. A. Rezayi, E. H. Skyrmions and the crossover from the integer to fractional quantum Hall effect at small Zeeman energies. Phys. Rev. B 47, 16419–16426 (1993)

[9] Meier, E., An, F. Gadway, B. Observation of the topological soliton state in the Su–Schrieffer–Heeger model. Nat Commun 7, 13986 (2016). https://doi.org/10.1038/ncomms13986

[10] Chen, Xie; Gu, Zheng-Cheng; Wen, Xiao-Gang (2010). "Local unitary transformation, long-range quantum entanglement, wave function renormalization, and topological order". Phys. Rev. B. 82 (15). doi:10.1103/physrevb.82.155138

[11] W. P. Su, J. R. Schrieffer, and A. J. Heeger. Solitons in Polyacetylene. Phys. Rev. Lett. 42, 1698 (1979)

[12] Friederike Klauck, Matthias Heinrich, and Alexander Szameit, "Photonic two-particle quantum walks in Su–Schrieffer–Heeger lattices," Photon. Res. 9, A1-A7 (2021)

[13] Cardano, Filippo Maffei, Maria Massa, Francesco Piccirillo, Bruno de Lisio, Corrado Filippis, G.De Cataudella, Vittorio Santamato, Enrico Marrucci, Lorenzo. (2015). Dynamical moments reveal a topological quantum transition in a photonic quantum walk

[14] J. K. Asboth. Symmetries, topological phases, and boundstates in the one-dimensional quantum walk. Phys. Rev.B, 86:195414, Nov 2012

[15] S. E. Venegas-Andraca. Quantum walks: a com-prehensive review. Quantum Information Processing,11(5):1015–1106, 2012

[16] J. Wang and K. Manouchehri. Physical Implementationof Quantum Walks. Springer, 2013

[17] Dariusz Wiater, Tomasz Sowiński, and Jakub Zakrzewski. wo bosonic quantum walkers in one-dimensional optical lattices. Phys. Rev. A 96, 043629 (2017)

[18] Asbóth, J.K., Oroszlány, L., Pályi, A. (2016). The Su-Schrieffer-Heeger (SSH) Model. In: A Short Course on Topological Insulators. Lecture Notes in Physics, vol 919. Springer, Cham. https://doi.org/10.1007/978-3-319-25607-8_1

[19] Navketan Batra and Goutam Sheet. Understanding Basic Concepts of Topological Insulators Through Su-Schrieffer-Heeger (SSH) Model (2019). arXiv:1906.08435v1

[20] Z. G. Soos G. W. Hayden (1988) Dimerization and Peierls Instability in Polyacetylene, Molecular Crystals and Liquid Crystals Incorporating Nonlinear Optics, 160:1, 421-432, DOI: 10.1080/15421408808083036

[21] Philipp M. Preiss and Ruichao Ma and M. Eric Tai and Alexander Lukin and Matthew Rispoli and Philip Zupancic and Yoav Lahini and Rajibul Islam and Markus Greiner. Strongly correlated quantum walks in optical lattices. Science 2015. https://doi.org/10.1126/science.1260364

[22] Travaglione, Ben. (2002). Implementing the quantum random walk. Phys. Rev. A. 65. 10.1103/PhysRevA.65.032310.

[23] Portugal, R. (2018). *Introduction to Quantum Walks. Quantum Walks and Search Algorithms*, 19–40. doi:10.1007/978-3-319-97813-0

[24] Abramowitz M and Stegun I A 1972 Handbook of Mathematical Functions (New York: Dover)

[25] Phillip Weinberg, Marin Bukov. QuSpin: a Python Package for Dynamics and Exact Diagonalisation of Quantum Many Body Systems part I: spin chains. arXiv:1610.03042 [physics.comp-ph](2017)

[26] Winkler, K., Thalhammer, G., Lang, F. et al. Repulsively bound atom pairs in an optical lattice. Nature 441, 853–856 (2006). https://doi.org/10.1038/nature04918

[27] Smith, A., Kim, M.S., Pollmann, F. et al. Simulating quantum many-body dynamics on a current digital quantum computer. npj Quantum Inf 5, 106 (2019). https://doi.org/10.1038/s41534-019-0217-0